Extended Abstracts of the 2012 International Conference on Solid State Devices and Materials, Kyoto, 2012, pp640-641

Effects of Thin Metal Insertion on Resistive Switching of Flexible ZnO RRAM

Cheng-Li Lin[1,a], Yi-Hsiu Lai[1,b], Syuan-Ren Yang[1], Chun-Ming Wu[1], Yao-Hsiang Yang[1], Chun-Hung Soh[1], Tze-Yu Lin[1], Chao-Fung Sung[2], and Pi-Chun Juan[3]

[1]Department of Electronics Engineering, Feng Chia University, No. 100, Wenhwa Rd., Seatwen, Taichung, Taiwan 407, R.O.C.
[2]Flexible Electronics Technology Division, Industrial Technology Research Institute (ITRI), Hsinchu, Taiwan 300, R.O.C.
[3]Department of Materials Engineering, Mingchi University of Technology, Taipei, Taiwan 243, R.O.C.
Phone: +886-4-24517250 Ext. 4969 Fax: +886-4-24510405 [a]E-mail: clilin@fcu.edu.tw; [b]E-mail: gpx06@hotmail.com

1. Instructions

Conventional charge-based memory will face the charge (data) loss problem when the feature size continues scaling down because of the number of stored electrons is decrease with feature size. Thus, new memory technology is necessary to develop for future application. Resistive RAM (RRAM) is one of the most promising candidates due to the simple structure (metal-insulator-metal, MIM), high density, and low power consumption [1,2]. Recently, flexible electronic attracts much attention and it will be the next generation and important technology [3,4]. In addition, the uniformity of resistance state of flexible RRAM will be degraded after long term switching or bending test. Thus, some improvements on the resistance switching such as thin metal insertion into the dielectric (switching layer) can improve the performance [5]. It is due to shortening the distance of conductive filament between metals [5,6]. Additionally, little study on the effects of various thin metal insertions on the switching layer. In this work, thin Zr, Ti or Zn metal is inserted into the ZnO oxide layer to investigate the characteristics of ZnO/thin-metal/ZnO RRAM deposited on flexible PEN substrate. The bending test and the switching mechanism are also investigated.

2. Experimental

The DuPont Q65 poly(ethylene 2,6-naphthalate) (PEN) substrate was used for the flexible substrate. First, the 4 cm × 4 cm PEN was cleaned with DI water, acetone and isopropanol using ultrasonic cleaner. Then 100-nm thick Al was deposited by dual E-Gun evaporator. Then, 25-nm-thick ZnO was deposited on Al bottom electrode. Three 5-nm-thick thin metal films of Zr, Ti and Zn were deposited on ZnO film, separately. After that, a 25-nm-thick ZnO was deposited on the thin metal. The ZnO film deposited using a ZnO target in a gas mixture of Ar and O_2 (24 and 12 sccm). After oxide thin film deposition, the top electrode of Al was deposited by dual E-Gun evaporator, and patterned by circular shadow mask with a diameter of 200 μm. **Fig. 1** shows the final structure of sample and the process steps. The physical photograph of the flexible RRAM sample is shown in **Fig. 2**. The electrical characteristics of the RRAMs were measured by an Agilent 4155C, including IV curve, endurance, retention, and mechanical bending test.

3. Results and Discussion

Fig. 3 shows the SEM plan view image of ZnO film deposited on various thin meal films. The grain size of ZnO film deposited on Zn thin metal shows the largest grain size (~ 47nm). The SEM of the 20-nm-thick ZnO film below the thin meal is shown in **Fig. 3(a)**, which grain size is similar to that of ZnO on Ti thin metal. Thus, the microstructure of ZnO film is depended on the under layer film. **Fig. 4** shows the I-V curves of various thin-metal insertions. The RRAM with Zn insertion reveals the highest HRS/LRS ratio and the largest switching cycles, but the variation of HRS is the largest. **Fig. 5** is re-plotted from the **Fig. 4** in logarithm scale. It shows the current transport behavior of ZnO RRAM with various thin-metal insertions. The slope of LRSs for three samples are near 1, which is the ohmic conduction [7,8]. The slopes of HRS at high voltage are 1, 1.7, and 1.3 for Zr, Ti and Zn thin-metal insertion, respectively. The slopes of HRS of RRAM with Ti and Zn thin metal insertion are larger 1, which are attributed to the trap-controlled space charge limit current (SCLC) mechanism [9,10]. Additionally, the RRAM with Ti thin meal insertion reveals more deeper oxide traps conduction in the stack film.

Fig. 6 shows the endurance of each sample. Endurance cycle of Zr insertion sample is 67 with the smallest resistance ratio of HRS/LRS. The Ti insertion sample reveals 83 switching cycles with medium resistance ratio. The largest resistance ratio and switching cycles (959) are observed on Zn insertion sample. Thus, the Zn insertion sample reveals the superior switching cycle. **Fig. 7** shows cumulative distribution function (CDF) of LRS and HRS for the Zr, Ti, and Zn insertion samples. In comparison with the previous result [11], the resistance state is more stable on multi-layer structure. **Fig. 8** and **9** show the retention characteristics of RRAM without and with 0.1V constant voltage stress, respectively. The retention shows without degradation for all samples, and it can pass 10 years of lifetime projection. **Fig.10** and **11** show the box plot of the set/reset voltages and LRS/HRS, respectively. More stable resistance and small resistance ratio are observed on Zr insertion sample, but the resistance ratio is the largest for the Zn thin metal insertion sample. The characteristic of bending test of the flexible RRAM is measured by the homemade instrument, as shown in **Fig. 12**. The LRS without obvious variation, but for HRS with periodic variation on Zn and Zr insertion samples after 1000 times bending (tensile bending). The HRS variation of Zn metal inserted RRAM after bending test shows better characteristic. It indicates that Zn insertion sample possess stable mechanical endurance on bending test (tensile bending). **Fig. 13** shows the proposed schematic of switching mechanism model according from the results of SEM (**Fig.3)** and the single-oxide-layer RRAM with much branches filaments [12,13]. Due to the amount of the smaller grain size in Zr insertion are larger, results in the larger leakage current and smaller resistance ratio. In the other hand, larger grain size of ZnO is observed on the thin Zn metal insertion sample, leads to the less conducting paths, smaller leakage current (HRS) and larger resistance ratio. In addition, it suggests that the filament is easily formed and ruptured in the Zn insertion sample. Thus, the switching cycle of the Zn insertion RRAM is larger than that of Zr (or Ti) insertion one.

4. Conclusions

This work investigates the effects of Zr, Ti, and Zn metals inserted into the ZnO oxide for Al/ZnO/metal/ZnO/Al/PEN flexible RRAM. A large resistance ratio and low power consumption are observed on the Zn inserted ZnO RRAM, and the switching cycle is up to 959 times. For the flexible bending test, the ZnO RRAM with thin Zn metal insertion reveals superior bending times (tensile bending) up to 1000 times.

Acknowledgements

This work was supported by the National Science Council, ROC, under contract No. NSC 100-2221-E-035-015. We are also thankful to the Industrial Technology Research Institute (ITRI) for providing the flexible materials.

References

[1]K. M. Kim et al.,APL, 91, 012907 (2007). [2]D. S. Jeong et al., nanotechnology, 20, 375201 (2009). [3] K. Kinoshita et al., Solid State Electron. 58, 48 (2011).[4] S. Kim et al., IEEE EDL, 56, 696 (2009). [5] J. Song et al., Applied Physics Express, 3, 091101 (2010). [6] Z. Fang et al., IEEE Electron Device Letters (EDL), 32, 566 (2011). [7]X. Liu et al., Electrochem. Solid-State Lett., 14(1), 9 (2011). [8] S. Jung et al., JECS, 157(11),1042 (2010). [9]S. K. Hong et al., JAP, 110, 044506 (2011). [10]H. D. Kim et al., IEEE EDL 32(8), 1125 (2011). [11]C. L. Lin et al., Symp. on Nano Device Technology (SNDT), pp.39 (2012). [12] G. S. Park et al., APL, 91, 222103 (2007). [14] X. Guo et al., APL, 91, 133513 (2007).

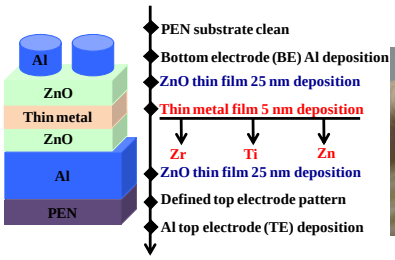

Fig. 1 The device structure and sample preparations of Al/ZnO/metal/ZnO/Al RRAM.

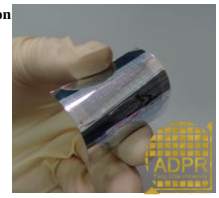

Fig.2 Photograph of flexible RRAM devices.

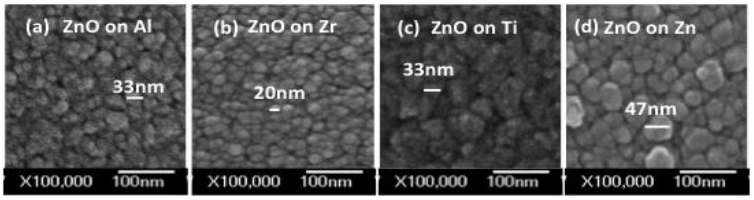

Fig. 3 SEM plane view images of ZnO film deposited on (a) Al (bottom electrode), and deposited on (b) Zr, (c) Ti, and (d) Zn thin-metal substrates.

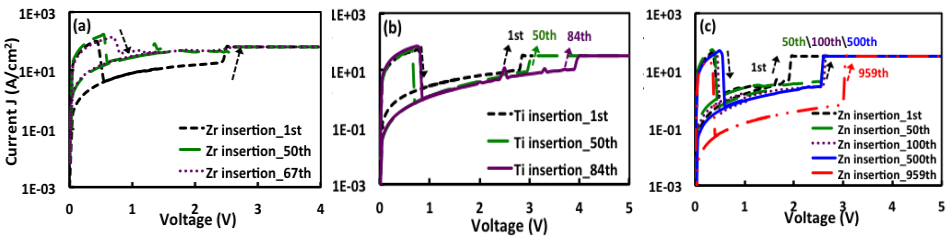

Fig. 4 Current versus voltage (I-V) characteristics with various switching cycles for (a) Zr insertion (b) Ti insertion and (c) Zr insertion. A current compliance of 1 mA is used for the dc sweep from HRS to LRS.

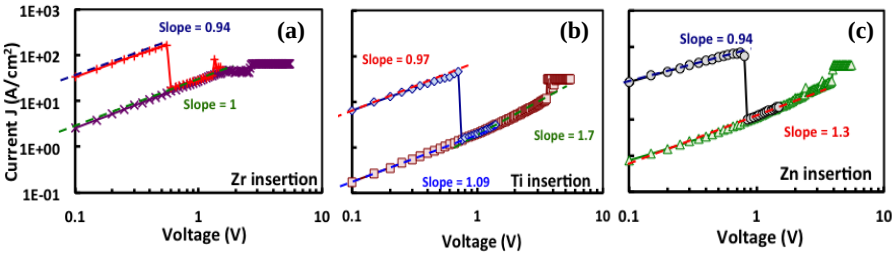

Fig.5 Current transport behavior of Al/ZnO/thin-metal/ZnO/Al RRAM with (a) Zr, (b) Ti and (c) Zn thin-metal insertion.

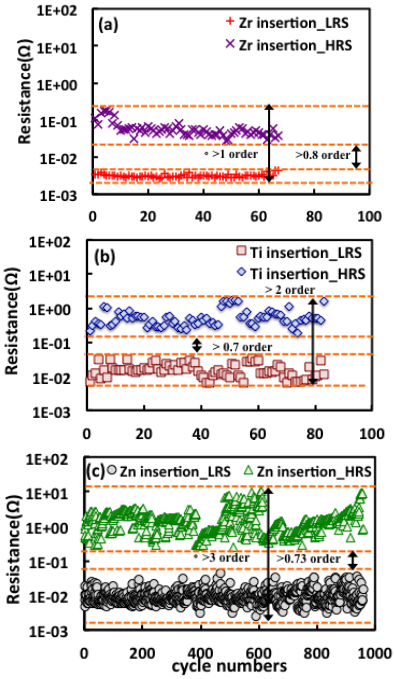

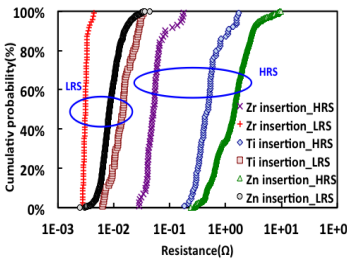

Fig.7 Cumulative distribution of high and low resistance state (HRS and LRS) of RRAM at 0.1V of reading voltage.

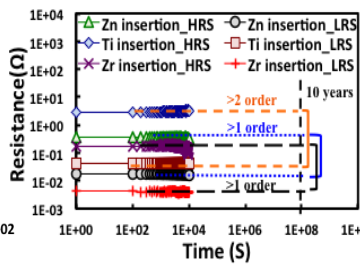

Fig.8 Retention characteristics of HRS and LRS of both structures at a reading voltage of 0.1V. No stress voltage was applied in retention measurement.

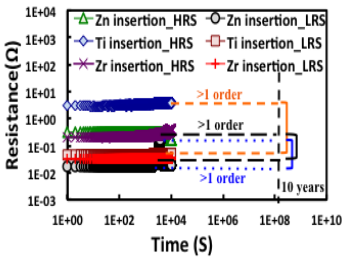

Fig.9 Retention characteristics of HRS and LRS of both structures at a reading voltage of 0.1V. The sample was stressed by 0.1V.

Fig.6 Switching endurance characteristics of Al/ZnO/metal/ZnO/Al RRAM for (a) Zr insertion (b) Ti insertion and (c) Zr insertion, and the endurance cycle is 67, 83, and 959 respectively.

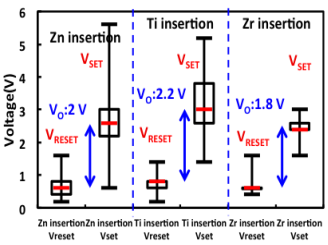

Fig.10 Box plot of the set/reset voltages of Al/ZnO/metal/ZnO/Al for (a) Zr (b) Ti, and (c) Zr insertion.

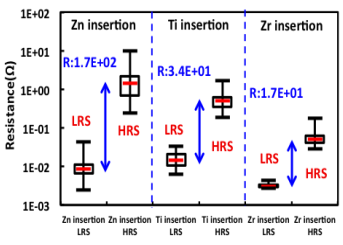

Fig.11 Box plot of the HRS and LRS of Al/ZnO/metal/ZnO/Al for (a) Zr (b) Ti, and (c) Zr insertion.

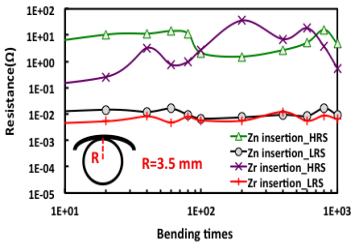

Fig.12 Mechanical endurance of Al/ZnO/metal/ZnO/Al on PEN substrate with Zn, Ti, and Zr insertion, respectively

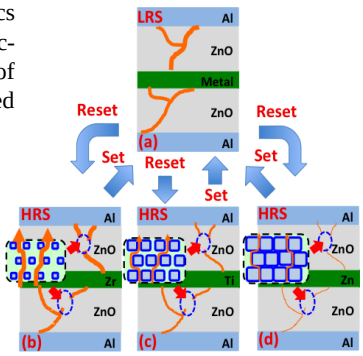

Fig.13 Schematic switching mechanism of Al/ZnO/metal/ZnO/Al RRAM for (b) Zr insertion (c) Ti insertion and (d) Zr insertion.